International Journal of Recent Technology and Engineering (IJRTE)
ISSN: 2277-3878 (Online), Volume-8 Issue-2, July 2019

FEA Simulation of Fluidic Based Pressure Sensor for Differrent Shaped Membrane

Muhammad Rashidi Ab Razak, Mohd Norzaidi Mat Nawi, Nur Shahira Shahripul Azeman, Mohd Faudzi Umar

Abstract*: In designing the fluidic based pressure sensor, the shape of the membrane is important in order to obtain maximum performance. The material used and the liquid inside the sensor is also important and deserve proper consideration. . In this work, the analysis of the membrane, materials and liquid using finite element analysis (FEA) are presented. The FEA simulation of the different shapes including square and rectangular shapes were carried out. The applied pressure and the dimension of selected membrane were varied in order to study the membrane performance.The result shows that the square shape produced the highest displacement of 4.7 mm compared to the other shapes. In terms of dimension, maximum performance can be achieved with a large area of membrane facing the applied pressure. The different types of membrane material andliquids that were used were also discussed. Two commonly used materials, Polyimide (PI) and Polydimethylsiloxane (PDMS) were chosen for this analysis. As for the liquids, methanol and propolyne carbonate were used.

***Index Terms*: Fluidic, FEA, Membrane.**

I. INTRODUCTION

There are many types of pressure sensor that are used in applications such as piezoresistive sensor, capacitive sensor, resonant sensor, pirani sensor and optical sensor [1]. Capacitive pressure sensor has been widely used in various types of applications including automotive, industrial and biomedical [2,3]. The advantages of using the capacitive are more compared to others. Some of the advantages include high resolution, a robust structure and lower power consumption [4,5]. The challenge of using the capacitive type sensor is the fabrication process for which silicon is the most commonly used the main material and it involves complex fabrication techniques such as deposition and layer etching [6]. Therefore, the fluidic technology was implemented in designing the pressure sensor.

A previous study proposes the use of the fluidic based pressure sensor as shown in Fig.1 by Nawi et. al.,[7]. It consists of circular shaped membrane, microchannel and sensing electrode. When pressure is applied on the top of the membrane, the liquid inside the microchannel is forced to flow. Fluidic technology offers a simple fabrication process and simple sensing technique that require a small amount of liquid to create the value capacitance [8]. Also, it has advantages in terms of damping characteristics where it is greatly enhanced to the external forces and is able to sustain considerable shock. Microfluidic technology in devices development has been widely used for various types of sensor, including pressure sensors, flow sensors and temperature sensors [9,10]. Commonly used materials in microfluidic system are Polyimide(PI) and Polydimethylsiloxane (PDMS). PI has high resistance against many chemicals, high glass transition temperature, high dielectric constant and biocompatibility [11]. Meanwhile, PDMS is one of the major materials used in polymer microfluidics because of material elasticity, and gas permittivity. In microfluidic based sensors, the output response depends on the liquid inside the channel. According to previous research, common liquids inside the microfluid sensors are methanol and propylene carbonate. The software used in, modelling related to shape structure and materials is the Finite Element Analysis ANSYS software. In this paper, we focus on the simulation of different shapes of membrane, variation of dimension and materials.

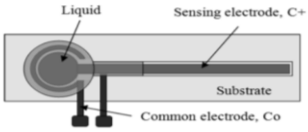

Fig. 1 Fluidic Based Pressure Sensor [7]

II. DESIGN AND METHODOLOGY

A. Simulation analysis using FEA

A simulation is used to find the select the suitable membrane shape based on the sensor performance. There are a few steps involved in the FEA simulation process for modelling structure. Fig. 2 shows the FEA simulation process.

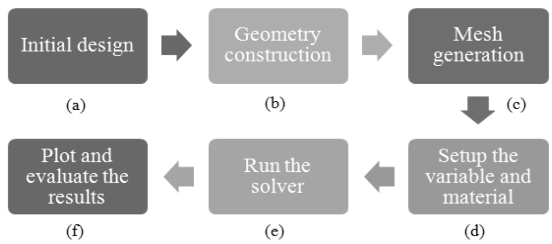

Fig. 2 FEA Simulation process. (a) design the sensor membrane. (b) construct a membrane structure. (c) Mesh is generated.

Revised Manuscript Received on 30 July 2019.

* Correspondence Author

Muhammad Rashidi Ab Razak*, Department of Physics, Universiti Pendidikan Sultan Idris, Perak, Malaysia.

Mohd Norzaidi Mat Nawi, Department of Physics, Universiti Pendidikan Sultan Idris, Perak, Malaysia.

Nur Shahira Shahripul Azeman, Department of Physics, Universiti Pendidikan Sultan Idris, Perak, Malaysia.

Mohd Faudzi Umar, Department of Physics, Universiti Pendidikan Sultan Idris, Perak, Malaysia.

(d) Set up the variable and material properties. (e) Run the solver to get the result (f) The data obtained are evaluated

The FEA simulation process is carried out in order to analyze and test the different shapes of membrane. The 3D geometry of square, and rectangular membrane are shown in Fig. 2. Table 1 shows the dimensions of each shape, where the area and thickness are fixed at 100 mm2 and 0.50 mm, respectively. Then, the mesh is generated in the design before setting up the variable. Each face of the design is assigned based on its function, such as input pressure and material. Data is obtained based on the results plotted after the solver finishes simulation.

Table 1. Dimension for different types of membrane shape

Type of membrane shape	Length, *a* (mm)	Width, *b* (mm)	Thickness (mm)	Surface Area (mm^2)
Square	10	10	0.5	100
Rectangular	5	20	0.5	100

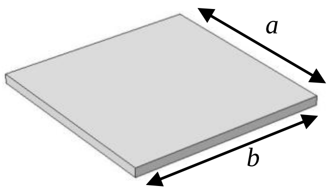

(a)

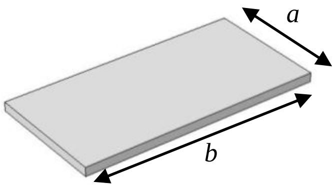

(b)

Fig. 3 Different shapes of membrane (a) Square shape, (b) Rectangular shape.

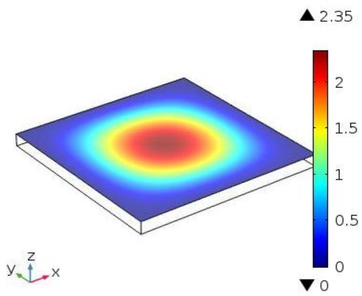

(a)

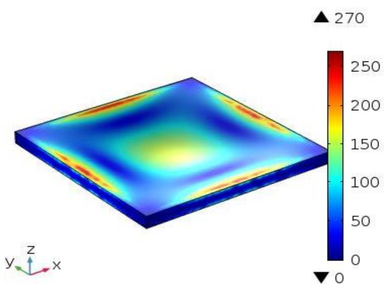

(b)

Fig. 4 Plotted contour for square shaped membrane (a) Displacement vector (b) Mises stress distribution.

The example of plotted contour for displacement and mises stress of square shaped membrane is shown in Fig. 4. The color indicates the different values for displacement as shown in Fig. 4 (a). At pressure 5kPa, the maximum displacement is 2.35 mm as shown in Fig. 4(a). The color indicates the different values at different points. The blue color indicates 0 mm of deflection due to a fixed position and red color indicates maximum deflection which is located in the middle of the membrane. Mises stress is also another parameter that can be accessed using the simulation. Mises stress is used in the simulation to check whether it is sustainable for membrane to be used based on the pressure range. According to Fig. 4(b), the maximum Mises stress value is 270 kPa.

B. Selection of Materials

Two different materials with suitable properties were used as the membrane for this analysis. The applied pressure is applied for PDMS and PI. PDMS is divided into three different properties which depend on the ratio of base solution and curing agent. There are two mechanical properties that were considered for this analysis, which includes Young's Modulus and poisson's ratio. The details of the material properties are listed in Table 2. Table 3 shows the details of liquids for methanol and propylene carbonate. The simulation was done by applied the pressure to produce fluid flow inside a microchannel with the dimensions of 800 μm x 800 μm that has a rectangular cross-section. The result in velocity was plotted and the comparison was made.

Table 2 The material properties for PDMS and PI [13]

PDMS (10:1)	Young's modulus (MPa)	0.85
	Poisson'ratio	0.5
PDMS (5:1)	Young's modulus (MPa)	1.00
	Poisson'ratio	0.5
PDMS (2:1)	Young's modulus (MPa)	2.10
	Poisson'ratio	0.5
PI	Young's modulus (MPa)	2500
	Poisson'ratio	0.34

Table 3 The liquid properties for methanol and propylene carbonate [14]

Liquids	Density (kg/m^3)	Dynamic viscosity (kg/ms)
Methanol	791.8	5.9×10^{-4}
Propylene carbonate	1205	2.0×10^{-3}

III. Result and Discussion

The findings were obtained through ANSYS Fluent 18.1. It has been discussed in detail based on the membrane displacement for variation of shapes, dimensions and materials.

A. FEA Simulation

Three different shapes of membrane was simulated using the ANSYS Fluent 18.1 and the results were obtained. Two different structures, which are square, and rectangular had been created to be tested based on applied pressure. Fig. 5 shows the findings of the drag force acting on different types of structures. The pressure within the range 0 to 10 kPa was applied on the top surface of the membrane and the result was recorded. Fig. 5 shows the graph for two shapes from which we can observe that the displacement had increased as the pressure increased. The square shape produced the highest deflection compared to the rectangular and circular shapes. Therefore, the square shape membrane was chosen for the next analysis.

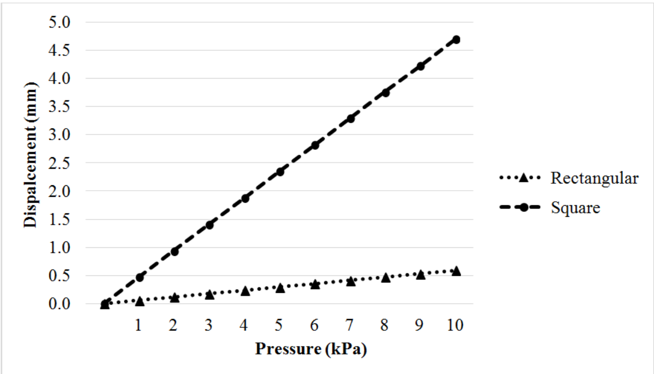

Fig 5 Displacement-pressure for different types of shape

Next, the dimensions of the square shape membrane was varied. The area of membrane within the range 60- 100 mm2 was selected for this analysis. Fig. 6 shows the plotted graph for the membrane displacement with respect to pressure for different areas. As expected, the highest performance of the sensor with larger area, which produced maximum displacement. In addition to that, the larger area, 100mm2 produced the highest displacement which was 4.6976 mm..

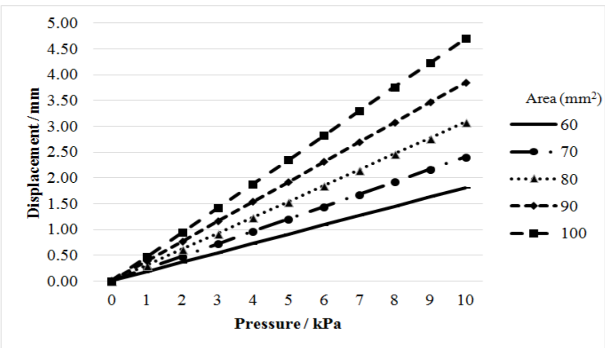

Fig. 6 Displacement-pressure of square shape membrane for different areas

B. Evaluation of Sensor Performance

The material properties as listed in Table 2 was used for the square shape membrane. A variation of the pressure was applied for different material, including PDMS with different ratio and Polyimide (PI). Fig. 7 shows the deflection of the membrane versus pressure. The membrane of PDMS (10:1) material produced a higher displacement compared to the others. The maximum value of deflection is 6.5 mm. Meanwhile. the PI material produced the lowest deflection which is 0.0035 mm. Which shows that PDMS (10:1) is more sensitive than PI.

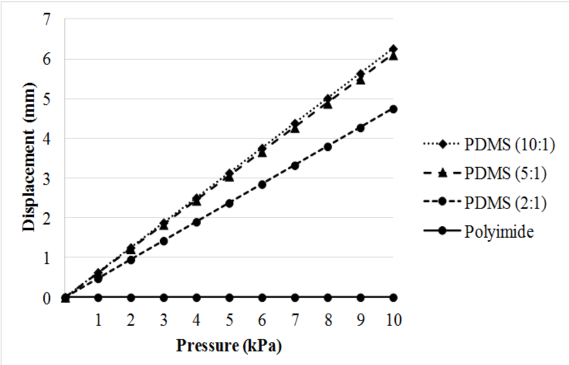

Fig. 7 Displacement-pressure for different materials

For the next analysis, the applied pressure was fixed at 5 kPa, while the dimensions, including area and thickness were changed. The PDMS material was used for this simulation. Fig. 8(a) shows the membrane displacement. As expected, the larger area with the smallest thickness give the maximum performance of membrane displacement. However, the selection of final dimension must consider the limitation of the fabrication process. Besides that, the mises stress is recorded to study the sensor limitation. Fig. 8(b) shows that the highest mises stress was 1.26 x 107 N/m2 for the largest area and smallest thickness. However, the PDMS membrane cannot be broken or damaged during pressure measurement, because the tensile strength of PDMS is 2.24 Mpa [15]. Although, the thinness of the membrane produces highest displacement,) it can still rupture when taken out over covering during the fabrication process[7]. In this simulation, the liquid is simulated inside microchannel 800 µm x 800 µm. We consider the steady laminar flow of an incompressible fluid with constant properties inside the microchannel. The moving liquid is forced to flow due to the membrane displacement. As predicted, the velocity increased as the pressure increased as shown in Fig. 9. The comparison was made between methanol and propylene carbinate where it showed that methanol has a better performance may be due to viscosity. As presented in Table 3, the viscosity of methanol is lower than propylene carbonate. For the next stage, the methanol was selected.

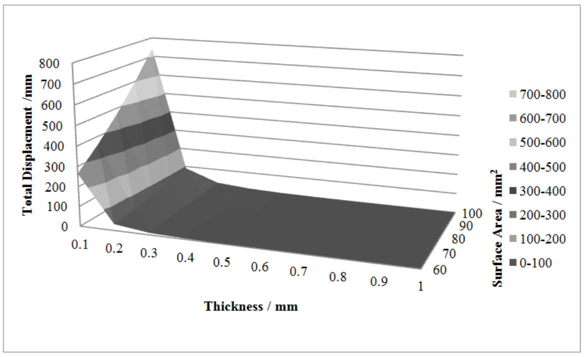

(a)

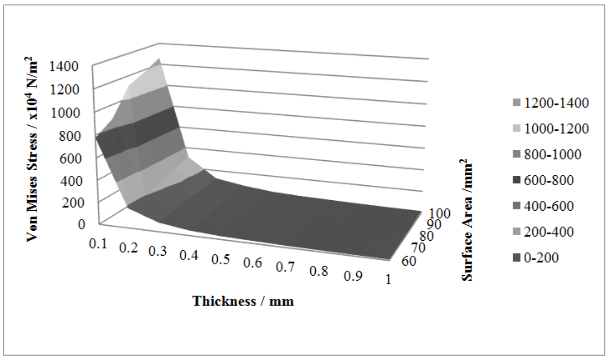

(b)

Fig. 8 The performance of membrane (a) displacement (b) Mises stress

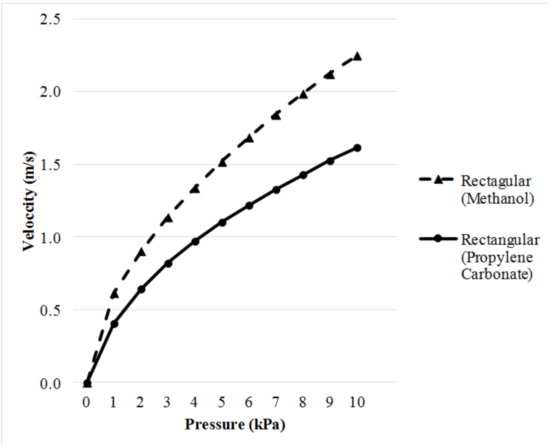

Fig. 9 Velocity of liquid based on the pressure applied for methaol and propylene carbonate

IV. Conclusion and Future Scope

FEA analysis of fluidic based pressure sensor was successfully simulated. The result showed that the square shaped structure produced a higher value of displacement compared to the rectangular shaped structure based on applied pressure. The PDMS with ratio 10:1 was selected for the sensor materials due to its high performance compared to others. The highest performance of the sensor was achieved by choosing the largest area and smallest thickness. However, it depends on the fabrication limition which will be the next scope of our work.

ACKNOWLEDGMENT

This work was supported by FRGS grant (2017-0077-101-02) and UPSI University Research Grant (2016-0180-102-01).

REFERENCES

1. Yunus, N. A. M., Halin, I. A., Sulaiman, N., Ismail, N. F., & Sheng, O. K. (2015). Valuation on MEMS Pressure Sensors and Device Applications. *International Journal of Electrical, Computer, Energetic, Electronic and Communication Engineering*, 9(8).
2. Almassri, A. M., Wan Hasan, W. Z., Ahmad, S. A., Ishak, A. J., Ghazali, A. M., Talib, D. N., & Wada, C. (2015). Pressure sensor: state of the art, design, and application for robotic hand. *Journal of Sensors*, 2015.
3. Xu, F., Li, X., Shi, Y., Li, L., Wang, W., He, L., & Liu, R. (2018). Recent developments for flexible pressure sensors: A review. *Micromachines*, 9(11), 580.
4. Eswaran, P., & Malarvizhi, S. (2012, March). Sensitivity analysis on mems capacitive differential pressure sensor with bossed diaphragm membrane. In 2012 *International Conference on Devices, Circuits and Systems (ICDCS)* (pp. 704-707). IEEE.
5. Bakhoum, E. G., & Cheng, M. H. (2009). Capacitive pressure sensor with very large dynamic range. *IEEE Transactions on Components and Packaging Technologies*, 33(1), 79-83..
6. Erguri, A. S., Huang, Y., Zhuang, X., Oralkan, O., Yarahoglu, G. G., & Khuri-Yakub, B. T. (2005). Capacitive micromachined ultrasonic transducers: Fabrication technology. *IEEE transactions on ultrasonics*, ferroelectrics, and frequency control, 52(12), 2242-2258.
7. Nawi, M. N. M., Manaf, A. A., Rahman, M. F. A., Arshad, M. R., & Sidek, O. (2014). One-side-electrode-type fluidic-based capacitive pressure sensor. *IEEE Sensors Journal*, 15(3), 1738-1746.
8. Nguyen, N. T., Hejazian, M., Ooi, C., & Kashaninejad, N. (2017). Recent advances and future perspectives on microfluidic liquid handling. *Micromachines*, 8(6), 186.
9. Rahman, M. F. A., Arshad, M. R., Manaf, A. A., & Yaacob, M. I. H. (2011, September). Modelling of a novel design of microfluidic based acoustic sensor. In 2011 *IEEE Regional Symposium on Micro and Nano Electronics* (pp. 56-59). IEEE.
10. Elbuken, C., Glawdel, T., Chan, D., & Ren, C. L. (2011). Detection of microdroplet size and speed using capacitive sensors. *Sensors and Actuators A: Physical*, 171(2), 55-62.
11. Zulfiqar, A., Pfreundt, A., Svendsen, W. E., & Dimaki, M. (2015). Fabrication of polyimide based microfluidic channels for biosensor devices. *Journal of Micromechanics and Microengineering*, 25(3), 035022.
12. Tsao, C. W. (2016). Polymer microfluidics: Simple, low-cost fabrication process bridging academic lab research to commercialized production. *Micromachines*, 7(12), 225.
13. Park, J. Y., Yoo, S. J., Lee, E. J., Lee, D. H., Kim, J. Y., & Lee, S. H. (2010). Increased poly (dimethylsiloxane) stiffness improves viability and morphology of mouse fibroblast cells. *BioChip Journal*, 4(3), 230-236.
14. Manaf, A. B. A., Nakamura, K., & Matsumoto, Y. (2008). Characterization of miniaturized one-side-electrode-type fluid-based inclinometer. *Sensors and Actuators A: Physical*, 144(1), 74-82.
15. Mark J.E., Ed., Polymer Data Handbook, vol. 2. New York, NY, USA: Oxford Univ. Press, 2009.